Neuro-Oncology Advances
6(1), vdae175, 2024 | https://doi.org/10.1093/noajnl/vdae175 | Advance Access date 24 October 2024

In situ optical feedback in brain tumor biopsy: A multiparametric analysis

Elisabeth Klint, Johan Richter, Peter Milos, Martin Hallbeck, and Karin Wårdell

All author affiliations are listed at the end of the article

Corresponding Author: Elisabeth Klint, MSc, Department of Biomedical Engineering, Linköping University, 58185 Linköping, Sweden (elisabeth.klint@liu.se).

Abstract

Background. Brain tumor needle biopsy interventions are inflicted with nondiagnostic or biased sampling in up to 25% and hemorrhage, including asymptomatic cases, in up to 60%. To identify diagnostic tissue and sites with increased microcirculation, intraoperative optical techniques have been suggested. The aim of this study was to investigate the clinical implications of in situ optical guidance in frameless navigated tumor biopsies.

Methods. Real-time feedback on protoporphyrin IX (PpIX) fluorescence, microcirculation, and gray-whiteness was given before tissue sampling (272 positions) in 20 patients along 21 trajectories in total. The primary variables of investigation were fluorescence in relation to neuropathological findings and gadolinium (Gd) enhancement, increased cerebral microcirculation in relation to bleeding incidence, number of trajectories, and impact on operation time.

Results. PpIX fluorescence was detected in Glioblastoma IDH-wildtype CNS WHO grade 4 ($n = 12$), Primary diffuse large B-cell lymphoma ($n = 3$), astrocytoma IDH-mutated CNS WHO grade 4 ($n = 1$) (Ki67 indices ≥ 15%). For 2 patients, no PpIX fluorescence or Gd was found, although samples contained tumorous tissue (Ki67 index 6%). Increased microcirculation was found along 9 trajectories (34 sites), located in cortical, tumorous, or tentorium regions. Postoperative bleedings ($n = 10$, nine asymptomatic) were related to skull opening or tissue sampling. This study strengthens the proposed independence from intraoperative neuropathology as PpIX fluorescence is detected. Objective real-time feedback resulted in fewer trajectories compared to previous studies indicating reduced operation time.

Conclusions. The integrated optical guidance system provides real-time feedback in situ, increasing certainty and precision of diagnostic tissue before sampling during frameless brain tumor biopsies.

Key Points

- In situ optical guidance increases certainty of diagnostic material during brain tumor needle biopsies.
- 5-ALA response enhances independence from intraoperative neuropathology.
- Multiparametric analysis suggests a Ki67 index threshold for fluorescence detection.

Brain tumor treatment relies on correct diagnosis posed by neuropathological analysis of representative tissue samples. Although needle biopsy procedures have a negative biopsy rate of approximately 5%,[1] they are associated with nondiagnostic or biased sampling in up to 25% of interventions.[2–5] Khatab et al. argue for a redefinition of the often-reported diagnostic yield to include certainty and precision of the diagnosis. Their redefinition aims to better address the number of biopsy cases where a definitive diagnosis including tumor type and grade cannot be posed.[6] In addition to

Importance of the Study

This study presents clinical implications of in situ optical feedback during needle biopsy integrated to the clinical procedure and postoperative multiparametric analysis from a single center. Feedback on protoporphyrin IX (PpIX) fluorescence, microcirculation, and gray-whiteness was given in real time before tissue sampling. PpIX fluorescence was detected in high-grade gliomas and lymphomas with strong correlation with gadolinium contrast enhancement. Increased microcirculation was found in cortical, tumorous, and tentorium regions. The present study strengthens independence from intraoperative neuropathology as PpIX peaks are detected. The integrated system resulted in fewer trajectories compared to previous studies indicating reduced operation time. The multiparametric analysis suggests a Ki67 index threshold for PpIX detection. In conclusion, the integrated optical guidance system provides real-time feedback in situ, increasing certainty and precision of diagnostic tissue before sampling during frameless brain tumor biopsies.

the redefinition, intraoperative techniques have been suggested to increase the diagnostic yield.[7,8]

A well-documented technique indicative of high-grade tumor tissue is 5-aminolevulinic acid (5-ALA)-induced fluorescence[4,5,9,10] often used during resection. Similar to fluorescence-guided resection (FGR), fluorescence feedback can be given for needle biopsies by placing the sampled tissue under a blue-light microscope.[11,12] If fluorescence is detected, studies suggest decreased dependency on intraoperative neuropathology[9] and shortened procedure time.[10] However, the fluorescence feedback is given after the tissue has been sampled, thus, the risk of sampling nondiagnostic tissue is unchanged. An alternative method is to measure fluorescence in situ. Our group has previously developed a probe-based optical measurement system for brain tumor biopsies allowing feedback on 5-ALA-induced fluorescence before tissue sampling.[13]

Needle biopsy procedures also come with the risk of hemorrhage,[1,14,15] both as the needle is inserted toward the tumor, and during tissue sampling. Thus, identification of increased blood flow sites has been suggested.[16,17] In the probe-based measurement system, an estimation of microcirculation and gray-whiteness of the tissue with laser Doppler flowmetry (LDF)[18] was integrated. Previously, the system was evaluated in 20 patients undergoing frame-based needle biopsies.[19] Since then, system improvements have been made and the probe has been further integrated into the clinical procedure by fitting the probe into the outer cannula of the biopsy needle, on which an aperture was made at the tip. The aperture allows for forward-looking measurements of fluorescence, microcirculation, and gray-whiteness in untouched tissue as the needle is inserted. The integrated setup was introduced in a smaller patient cohort for frame-based[20] and frameless[21] navigation procedures, respectively. However, the investigational system and its clinical potential have not been evaluated in a larger cohort.

Therefore, the aim of this work was to investigate the clinical implications of optical guidance in frameless navigated brain tumor needle biopsies. The primary variables of investigation were fluorescence in relation to neuropathological findings and MRI contrast enhancement, increased cerebral microcirculation in relation to bleeding incidence, and impact on operation time. First, in situ optical measurements were recorded and displayed in real time during surgery. Second, postoperative multiparametric analysis was conducted where the optical data were combined with frameless neuronavigation data, postoperative imaging, and detailed neuropathological analysis through digital pathology. The work was conducted as a prospective, single-center study.

Methods

Patients

Twenty patients (68 ± 14 years, 7 females) were included in the study. The inclusion criteria were adults with suspected high-grade glioma on preoperative MRI not eligible for resection. All patients were planned for needle biopsy at Linköping University Hospital. Tumors were located in the frontal, fronto-temporal, temporal, and fronto-parieto-occipital regions.

The study was approved by the Swedish Ethical Review Authority (EPM2020-01404). Each patient gave written informed consent before inclusion.

An oral dose of 5-ALA (Gliolan®, 20 mg/kg [18.5 ± 1.5 mg/kg], Medac GmbH, Germany) was given to each patient 2–3 h before surgery according to the clinical routine for FGR.[11] Average time from administration to measurement was 04:45 ± 00:50 (hh:mm).

Optical Measurement System

The investigational measurement system is illustrated in Figure 1 and described in detail in refs. [21,22]. In short, the setup consists of 2 modules, one for fluorescence spectroscopy, and one for LDF (PF 5000, Perimed AB) measurements. Light from 2 laser sources (405 nm—fluorescence and 780 nm—LDF) is transmitted through 2 optical fibers in the probe to the tissue. The backscattered light is transmitted back through optical fibers to the spectrometer and photodetector. Recorded signals are collected from tissue immediately in front of the probe tip. Signals are displayed in real time in the in-house software (Figure 1). Fluorescence spectra are acquired in groups of 3 in the range 450–750 nm. Perfusion (microcirculation) and total light intensity (TLI, gray-whiteness) signals are acquired continuously in the ranges 0–1000 arbitrary units (a.u.) and 0–10 a.u., respectively.

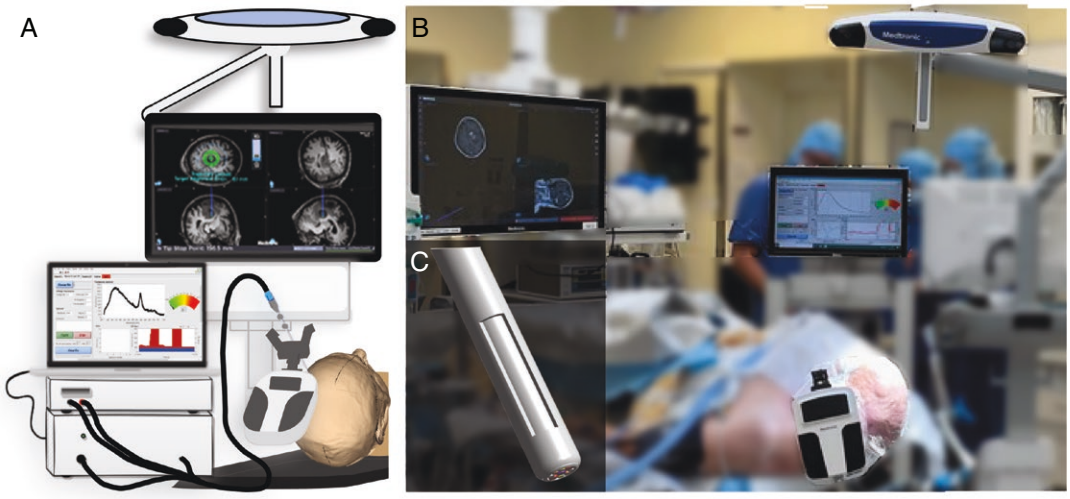

Figure 1. (A) Schematic of the investigational measurement setup. From the left: optical measurement system, navigation system, AutoGuide® holding the probe-needle kit in place above the patient. During surgery, the measurement system is placed outside of the sterile zone. The spectrum on the screen shows a protoporphyrin IX peak. (B) Setup in the operating room. (C) Schematic of the modified probe-biopsy needle kit.

Image Acquisition

Before surgery, a clinical navigation protocol (voxel size $1 \times 1 \times 1$ mm^3) was acquired on an MRI scanner ($n = 18$ on 3T Siemens Healthineers or Philips, $n = 2$ on 1.5T Philips or GE Healthcare, depending on scanner availability) with and without Gadolinium (Gd) contrast. After surgery, CT (SOMATOM, Siemens Healthineers) was acquired if there was a clinical need, for example, suspected bleeding, otherwise, MRI was acquired.

Needle Biopsy With Optical Guidance

The routine needle biopsy procedure was carried out with the addition of optical measurements during needle insertion. A detailed description of the procedure is found in ref.[21]. In short, planning and registration are made using the navigation system (StealthStation S8, Medtronic Inc.). A burr hole of 3.2 or 10 mm is made in the skull and the dura is opened. The biopsy needle (Passive Needle Kit, Medtronic Inc.) with the probe inside is held in place by the AutoGuide® (Medtronic Inc.). The probe-needle kit is manually inserted in steps of a few millimeters, pausing for 5–10 s in each position for signal acquisition. Measurements are acquired at the probe tip and signals are displayed in real time. Increased microcirculation spots, protoporphyrin IX (PpIX) peaks, navigation coordinates, and acquisition time points are noted. When in proximity of the planned target, if PpIX peaks are detected, the highest peak is located, and the needle window adjusted to overlap the corresponding tissue volume. Then, the probe is replaced by the inner cannula of the biopsy needle and tissue samples are taken according to clinical routine (4 directions, separated by a 90-degree rotation of the needle). If the surgeon deems the tissue material too sparse, the needle is adjusted a few millimeters, and a second biopsy sampling is made. Finally, the patient is prepared for the end of surgery while waiting for the intraoperative neuropathological evaluation. If no PpIX peak is found, the clinical routine is followed, i.e., tissue samples are taken in the preoperative target position and the surgery is paused until a response from the neuropathologist is received, before preparing the patient for the end of surgery.

Neuropathological Diagnosis

Intraoperative neuropathological evaluations were done on Hematoxylin and Eosin (H&E) stained fresh smears and/or frozen sections. The remaining material was subsequently formalin-fixed and paraffin-embedded. Tissue sections (3 µm) were subject to deparaffinization and heat-induced epitope retrieval. Sections were stained with H&E and Ki67. Stained slides were digitalized for evaluation. Molecular analysis was performed using Therascreen IDH1/2 RGQ PCR kit (QIAGEN) and Therascreen MGMT Pyro kit (QIAGEN) according to the manufacturer's instructions. Selected cases were also analyzed with massive parallel sequencing using the Genomic Medicine Sweden 560 panel for solid tumors (GMS560). The integrated diagnosis was done according to the fifth edition of the WHO classification of CNS tumors.[23] The final clinical diagnosis was given within 2 weeks of surgery.

It should be noted that, in this study, "high-grade" refers to tumors with morphological growth patterns of CNS WHO grade 3 or 4 tumors. Similarly, "low-grade" refers to morphological growth patterns of CNS WHO grade 2 tumors.

Data Analysis

In addition to the clinical diagnosis, a detailed reevaluation of all samples was made by a senior neuropathologist (M.H.).

The reevaluation was made on scanned digital neuropathology images viewed in Sectra workstation, IDS7 (Sectra AB) and included coarse percentages of high- and low-grade tumor tissue, necrosis, and non-tumor tissue. Ki67 index was digitally quantified using the nuclear detection algorithm of IDS7.[24] Relevant molecular analyses, for example, isocitrate dehydrogenase (IDH) mutations and O^6-methylguanine-DNA-methyltransferase (MGMT) methylation, were also reported.

Tissue fluorescence was represented both by the entire spectrum and by PpIX-peak height at 635 nm after correction for autofluorescence contribution. To separate signal from noise, the autofluorescence was normalized for each spectrum and a signal-to-noise ratio (SNR) of 5:1 was applied. If the SNR was lower than 5, the spectrum was discarded. The continuous perfusion and TLI signals were represented by the average and standard deviation over the 5–10 s interval in each position. Increased microcirculation spots were identified, defined as perfusion > 100 a.u., which is twice the common value (< 50 a.u.) in white matter.[18] The TLI signal trends were summarized as a pair of arrows for each patient. TLI values < 0.5 a.u. indicate that an insufficient amount of light reached the detector, thus the perfusion value was set to zero in these cases.

For the multiparametric analysis, all imaging, navigation, and optical data were registered to and presented in the T_1wGd image space used for navigation as previously described.[21] The final entry point in the skull (CT) or dura (MRI), and the biopsied position were identified on postoperative imaging. Then, the planned and final measurement positions were compared by Euclidian distance.

Results

In total, 21 trajectories and 272 measurement positions were probed. PpIX findings in the biopsy region were corroborated by Gd contrast enhancement. PpIX fluorescence and Gd were present in the biopsy region of 16 patients (17 trajectories), and absent in 4 patients. A summary of the findings for each patient is presented in Table 1. No adverse events or side effects related to the administration of 5-ALA were reported.

Neuropathology

In this cohort, 18 patients were diagnosed with tumors. More specifically, the diagnoses were 15 gliomas (13 Glioblastoma IDH-wildtype, CNS WHO grade 4; 1 Astrocytoma IDH-mutated, CNS WHO grade 4; 1 Glioma, IDH-wildtype, CNS WHO grade 2); 3 Primary diffuse large B-cell lymphoma of the CNS; and 2 non-tumor. For one patient, non-tumor tissue with increased astrocytic activity without signs of malignancy was found. The second non-tumor sample was confirmed on postoperative imaging to be off-target. Ki67 index varied from 6% to 54% for glioma and 90–99% for lymphoma cases. In the glioblastoma group, 6 were MGMT-methylated and 8 were unmethylated.

Fluorescence

PpIX fluorescence was found in the biopsy region in 16 patients, including 13 gliomas, and all 3 lymphomas. Example spectra from 4 patients are shown in Figure 2. In the biopsy region, fluorescence findings and Gd contrast enhancement were concordant (Figure 3A), with a Phi coefficient of 0.64 throughout the trajectories. Strong correlation was seen for glioma but not for lymphoma (0.72 and 0.18, respectively), and peak height was more prominent in glioma (Figure 2A, C, D) than in lymphoma (Figure 2B). For one additional patient, PpIX peaks (ratio: 0.11–0.14) were found along the trajectory, but not in the biopsy region (Figure 4C). After postoperative imaging and registration, these PpIX peaks and Gd enhancement were attributed to accumulation in the tentorium cerebelli. In < 2% of measurement positions (5 of 272), spectra were discarded due to low SNR. Fluorescence spectra and LDF signals for all patients are found in Figure A1 in Supplementary Appendix A.

Out of the 4 patients without PpIX fluorescence peaks in the biopsy region (Figure 4), 2 samples were non-tumorous, one diagnosed as a low-grade glioma (CNS WHO grade 2), and one glioblastoma (IDH-wildtype, CNS WHO grade 4). None of the 4 cases showed parenchymal Gd enhancement along the trajectory (Figure 3A). In the latter case, no necrosis or microproliferent vessels were found in the sample. Next-generation sequencing (NGS) revealed a mutation in the TERT-gene promotor and amplification of the epithelial growth factor receptor (EGFR). Ki67 index was 6% in both tumorous non-fluorescent, non-Gd cases (Table 1).

Tissue Microcirculation and Gray-Whiteness

Increased microcirculation (perfusion > 100 a.u.) was found in one or more sites along the trajectory of 9 patients (Table 1, Figure 3B), that is, in 34 out of 272 measurement positions. These were located in the cortical ($n = 14$), tumorous ($n = 7$), or tentorium ($n = 13$) regions on MRI. In 15 of the 34 positions, perfusion values were in the range 250–500 a.u. For one patient, 10 out of 19 positions showed increased perfusion > 250 a.u. (Figure 4C). Postoperative CT indicated that this trajectory went through the tentorium cerebelli. Here, postoperative imaging indicated an asymptomatic bleeding. In total, ten asymptomatic and one symptomatic bleeding were detected in 10 patients in total. Postoperative imaging confirmed bleedings to be associated with tissue sampling ($n = 9$), and opening of the skull ($n = 2$). In 2 positions, the TLI signal was below the detection threshold, see example at 1.2 mm past target in Figure 4C.

TLI signals generally increased (8 patients) or stayed constant (9 patients) from the entry point throughout the first half of the trajectory. These trends are related to passage from darker to lighter tissue, for example, from gray to white matter, or to passage through the same type of matter. In the second half of the trajectory, signals decreased (15 patients) or kept constant (5 patients). The decreasing trend indicates darker or more compact tissue, for example, gray matter or tumorous tissue.

Number of Trajectories and Measurement Time

A total of 21 trajectories were biopsied. Registration and targeting errors in the navigation system were 1.6 (± 0.3, $n = 12$) mm and 0.3 (± 0.2) mm, respectively. The median

Table 1. Fluorescence, Perfusion, TLI, and Neuropathology Results for Each Patient

Pat no	Fluo (+/-)	**Traj no (#)**	Meas points (#)	Fluo peaks (#)	**Incr. Perf (#)**	TLI	Meas time (min)	Response time (min)	Tumor location	**Sample classification (CNS WHO 2021)**	IDH status	MGMT status	Ki67 index (%)	Other molecular markers
1	+, +	2	33, 39	6, 15	8 (4), 0	↗→	21, 23	-	Insular, thalamic	Glioblastoma, grade 4	wt	met	25	
2	+	1	22	10	0	→↘	12	40	Insular, thalamic	Glioblastoma, grade 4	wt	unmet	54	
3	+	1	16	6	0	→→	6	45	Frontal, trigonal	Glioblastoma, grade 4	wt	met	52	
4	+	1	11	3	0	→↘	10	45	Trigonal, insular, thalamic	Primary diffuse large B-cell lymphoma of the CNS	-	-	93	
5	+	1	9	1	0	→↘	13	50	Bifrontal, periventricular, transcallosal, including splenium	Primary diffuse large B-cell lymphoma of the CNS	-	-	99	
6	-	1	10	0	3 (0)	↗↘	5	30	Temporo-occipito-medio-basal (RIGHT)	Glioma, grade 2	wt	-	6	
7	+	1	8	4	0	↗↘	4	-	Frontal, insular	Glioblastoma, grade 4	wt	unmet	39	
8	+	1	8	3	0	↗↘	4	-	Fronto-temporal, insular (RIGHT)	Glioblastoma, grade 4	wt	unmet	38	
9	+	1	11	3	2 (1)	→↘	6	50	Frontal, para- and intraventricular	Glioblastoma, grade 4	wt	unmet	15	
10	+	1	9	3	1 (0)	↘↘	4	60	Multilocular, frontopolar, insular (RIGHT)	Glioblastoma, grade 4	wt	unmet	50	
11	+	1	12	3	0	→↘	8	60	Frontal (RIGHT)	Primary diffuse large B-cell lymphoma of the CNS	-	-	90	
12	+	1	8	3	3 (0)	↗↘	12	45	Fronto-median (RIGHT)	Glioblastoma, grade 4	wt	met	24	
13	+	1	6	2	0	→↘	4	40, 50	Temporal	Glioblastoma, grade 4	wt	met	34	
14	-	1	10	0	0	→↘	5	30	Frontal, Insular (RIGHT)	Glioblastoma, grade 4	wt	met	6	Mutation in TERT-gene-promotor, EGFR amplification, no chromosome 7+/10– loss
15	-	1	19	2	13 (10)	↘→	19	30	Temporo-medio-basal	Non-tumor	-	-	-	
16	+	1	10	6	2 (0)	↗↘	7	60	Temporal, Insular	Astrocytoma, grade 4	mut	met	21	CDKN2A/2B homozygote deletion
17	-	1*	9	0	1 (0)	→→	5; 3	50, 50	Fronto-parieto-occipital, paraventricular	Non-tumor	-	-	-	
18	+	1	7	2	0	↗↘	5	25	Temporal	Glioblastoma, grade 4	wt	unmet	32	
19	+	1	5	3	0	↘→	6	35	Frontal (RIGHT)	Glioblastoma, grade 4	wt	unmet	46	
20	+	1	10	4	1 (0)	↗↘	10	35	Bifrontal, transcallosal	Glioblastoma, grade 4	wt	unmet	54	
Tot	**16**	**21***	**272**	**79**	**34 (15)**		**8 ± 5**	**44 ± 11**						

Abbreviations: ATRX = α-thalassemia/mental retardation syndrome X-linked; EGFR = epidermal growth factor receptor; Fluo = fluorescence; IDH = isocitrate dehydrogenase; incr = increased; meas = measurement; MGMT = O6-methylguanine-DNA-methyltransferase methylation; perf = perfusion; TERT = telomerase reverse transcriptase; TLI = total light intensity; traj = trajectory.
*The same trajectory was probed twice due to negative neuropathology response.

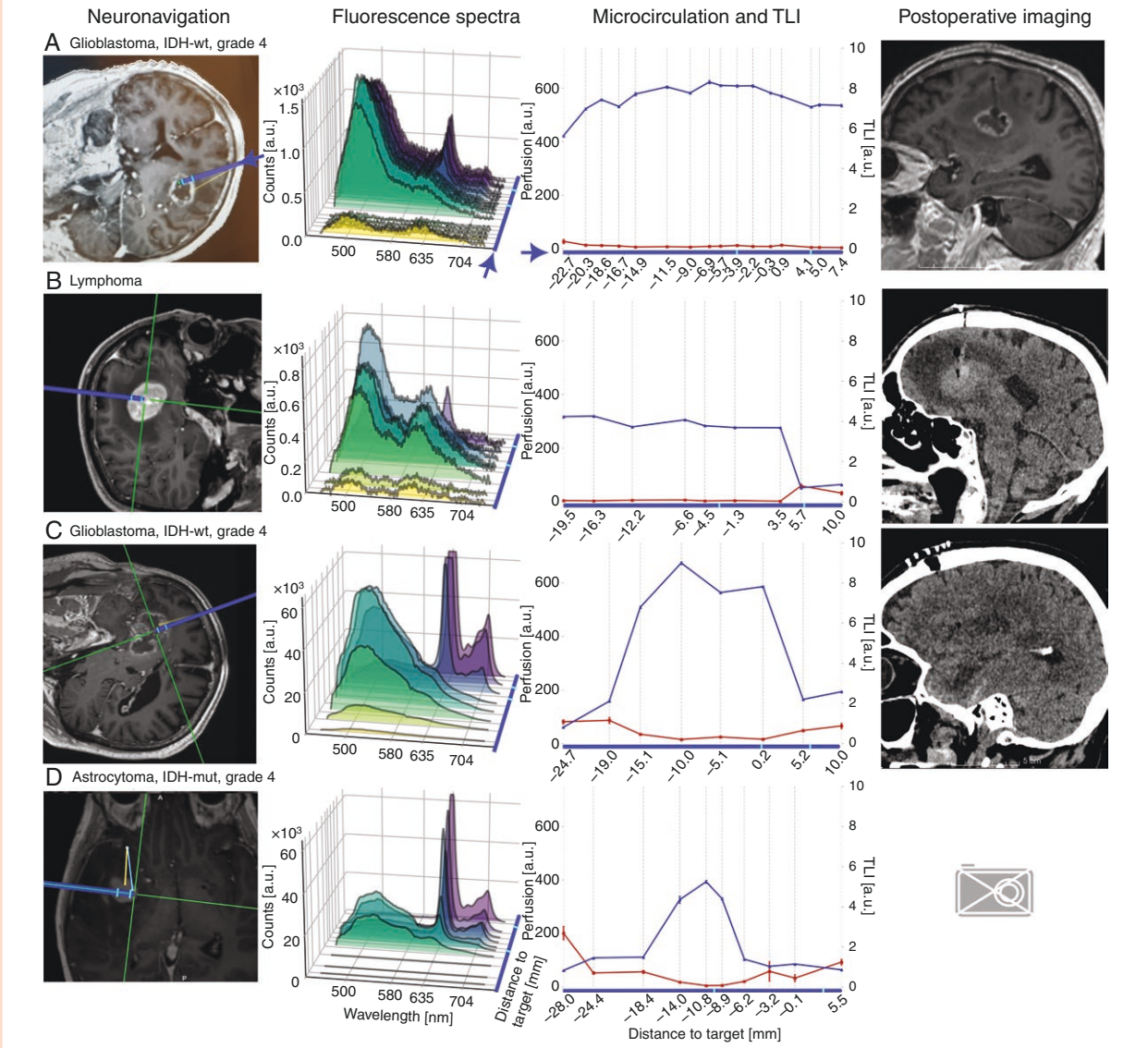

Figure 2. Imaging and optical data for (A) Patient 3, (B) Patient 5, (C) Patient 8, and (D) Patient 16 with positive fluorescence response in the biopsy region (Table 1). Left column: Preoperative imaging with superimposed intraoperative trajectory (indicated by the dark line). Middle column: optical data including fluorescence spectra, as well as average and standard deviation of perfusion and TLI signals along the trajectory. Arrows point in the direction of the needle trajectory. The pair of vertical lines perpendicular to the trajectory indicate the boundaries of the biopsy window. Right column: Postoperative imaging with final needle trajectory and biopsy position.

Euclidian distance between the planned and final positions was 2.8 mm (1.8–6.2 mm, $n = 13$). The average time for optical measurements along a trajectory including annotation time was 8 (± 5) min. The response time for the pathologist was 44 (± 11, $n = 17$) min.

Discussion

Multiparametric analysis was carried out in 20 neuronavigated frameless brain tumor needle biopsies, including a unique combination of in situ optical guidance, postoperative imaging, and detailed neuropathological analysis. The probe-based optical method allows seamless integration into the clinical workflow. Compared to the routine procedure, additional tissue impact is minimized while providing real-time feedback on PpIX fluorescence, microcirculation, and gray-whiteness before tissue is sampled. To our knowledge, this is the first study to compare in situ optical signals to postoperatively corrected MRI indications and tumor percentages from neuropathological findings in frameless neuronavigated biopsy patients.

Fluorescence in Gliomas and Beyond

Fluorescence response was in line with the neuropathological report in 18 patient cases. Diagnoses included Glioblastoma IDH-wildtype CNS WHO grade 4,

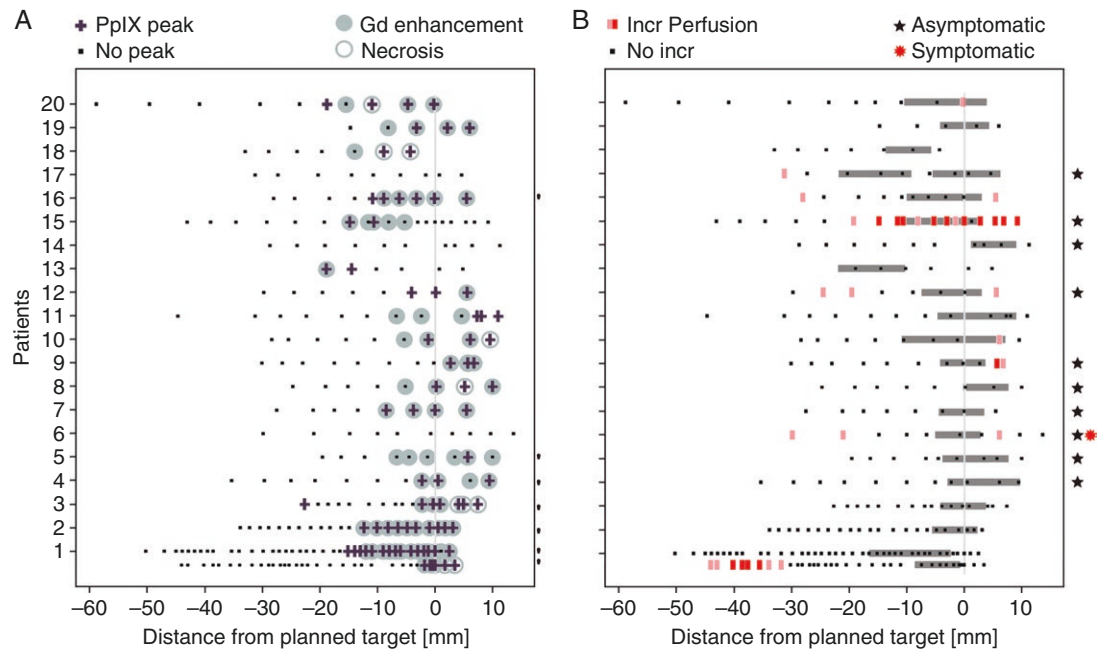

Figure 3. Optics and imaging findings in relation to the planned target. (A) PpIX fluorescence (crosses), gadolinium (Gd) contrast enhancement (filled circle) and intratumoral necrosis (hollow circle) on MRI. The gray line at 0 mm indicates planned target position. Patients 1–6, and 16 were assessed on preoperative imaging (′). (B) Increased perfusion (vertical lines, transparent >100 a.u., opaque >250 a.u.) and biopsy window (gray boxes) together with bleeding occurrence (star: asymptomatic, double star: symptomatic).

Astrocytoma IDH-mutant CNS WHO grade 4, Primary Diffuse Large B-cell Lymphoma, and non-tumor. This is in line with reports in literature where PpIX fluorescence first and foremost has been used in high-grade glioma FGR but has also been suggested as support for lymphoma identification.[25,26] All 3 lymphomas in our cohort showed positive fluorescence response in the biopsied volume compared to 8 out of 11[25] and 32 out of 40[26] in previous lymphoma-specific studies. Still, agreement between Gd contrast enhancement and fluorescence peaks was notably lower for lymphoma than for glioma. Beyond Gd, studies indicate a potential benefit of 5-ALA administration for non-enhancing tumors, as approximately 20% of cases fluoresce.[27] However, in this study, neither of the 2 non-enhancing tumors showed PpIX fluorescence.

Relation Between Fluorescence, Neuropathology, and Gadolinium Enhancement

A positive PpIX fluorescence response was associated with a Ki67 index of ≥ 15% (16 cases). The 2 tumorous samples with negative PpIX response had a Ki67 index of 6% and corresponded to a low-grade glioma, and a glioblastoma, respectively. Other studies have indicated a correlation between visible PpIX accumulation and Ki67 index.[27–29] In their 2021 study, Black et al. found "strong," "weak," and no fluorescence to be associated with proliferation indices of 24%, 29%, and 17%, respectively. Interestingly, Jaber and colleagues found that fluorescing gliomas were associated with a significantly higher Ki67 index than non-fluorescing tumors.[27] In the present study, non-fluorescing tumors were also associated with a lower Ki67 index, but due to the limited number of tumors of grades 2 and 3 in this cohort, no further attempts at correlations with WHO grade were made. Future studies should consider and further investigate the relation between Ki67, PpIX response, and tumor grade.

In addition, to Ki67 index, EGFR amplification has been associated with lower fluorescence response in several glioblastoma cell lines.[30] Fontana et al. attributed the lowered response to increased expression of heme oxygenase-1. In the current study, the non-enhancing, non-fluorescing glioblastoma sample did not contain any endothelial cell proliferent vessels or necrosis. Therefore, NGS was performed to conclude the diagnosis. Sequencing revealed EGFR amplification, TERT-gene-promotor mutation, and no chromosome 7+/10– loss confirming the glioblastoma diagnosis.[31,32] However, it should be noted that NGS was not deemed necessary for diagnosis for any other sample in this cohort, thus potential EGFR amplification is unknown for the other samples. EGFR amplification and its impact on PpIX fluorescence is of interest for future studies.

Positive fluorescence response was also associated with Gd and necrosis dominant voxels on MRI. Out of 18 locations with PpIX-fluorescence but no Gd enhancement, 10 were in direct proximity to enhancing areas. As the biopsy trajectory is not confined to the voxel grid of MRI, registration errors and contribution from several voxels could give rise to this discrepancy. On the other hand, PpIX accumulation has been indicated to extend beyond Gd on conventional MRI, which could also contribute to the increased fluorescence extent.

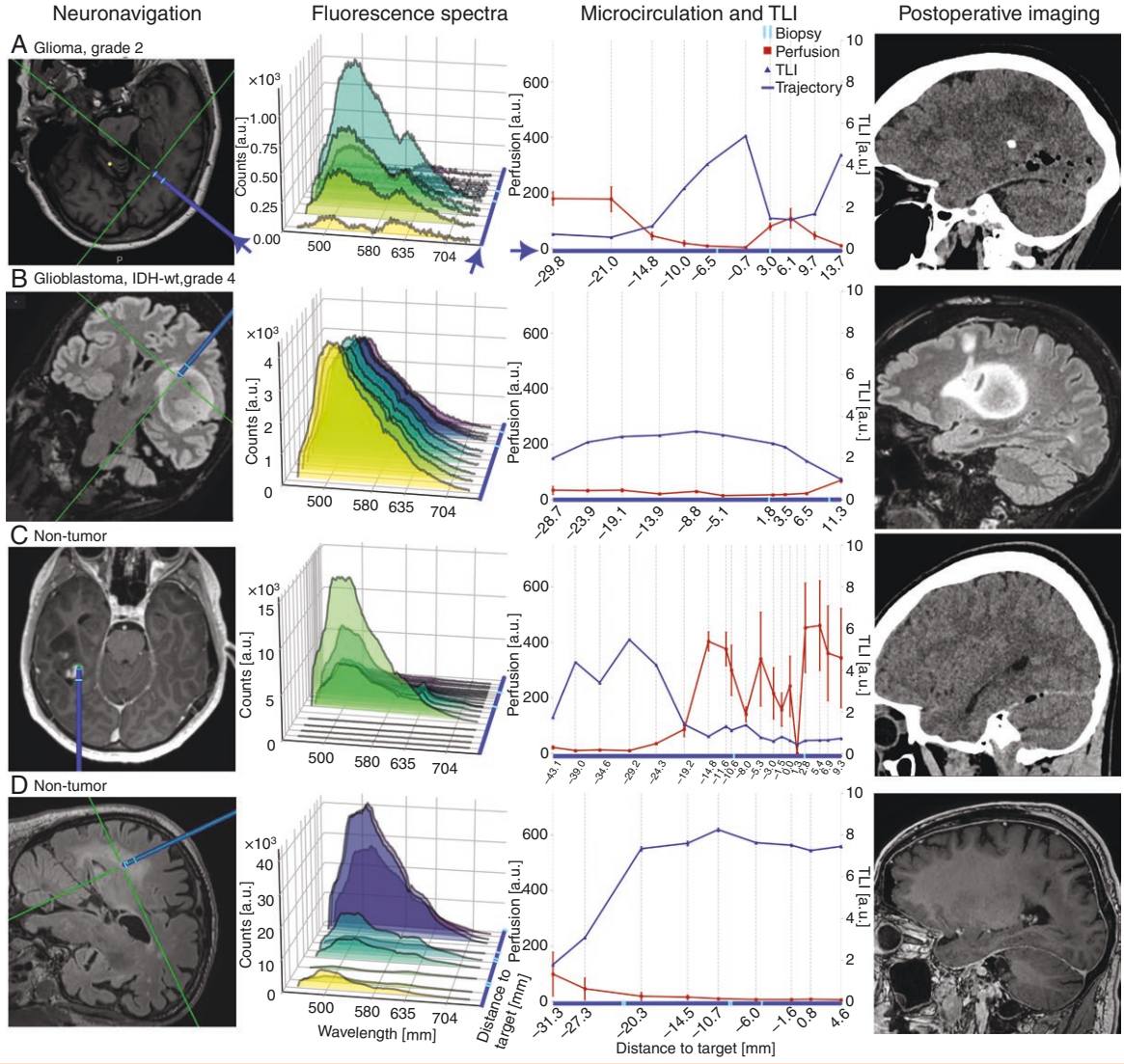

Figure 4. Imaging and optical data for (A) Patient 6, (B) Patient 14, (C) Patient 15, and (D) Patient 17 without PpIX fluorescence response in the biopsy region (Table 1). Left column: Preoperative imaging with superimposed intraoperative trajectory (indicated by the dark line) Patients A, B, and D, did not show gadolinium contrast enhancement. In (C) PpIX indications were found in tissue attributed to tentorium cerebelli on postoperative imaging. Middle column: optical data including fluorescence spectra, as well as average and standard deviation of perfusion and TLI signals along the trajectory. Arrows point in the direction of the needle trajectory. The pair of vertical lines perpendicular to the trajectory indicate the boundaries of the biopsy window. Right column: Postoperative imaging with final needle trajectory and biopsy position.

Independence on Intraoperative Neuropathology

Millesi et al.[9] argue that intraoperative neuropathology is not needed if fluorescence guidance is used. According to our study, this could, in extension, indicate a shorter procedure time. Herein, measurements took on average < 10 min while the average waiting time for the intraoperative response from the pathologist was 45 min. As PpIX peaks are identified, the operation time could be shortened by 35 min on average (range: 11–56 min) for the presented cohort. Two other studies also found a shortened procedure time when positive fluorescence was found.[9,10] Additionally, as surgical time is reduced, so are the costs.[9]

It should be noted that previous studies assessed tissue fluorescence under a blue-light microscope after sampling. On the contrary, the presented method allows fluorescence feedback before sampling, potentially decreasing the amount of tissue sampled. As an example, during the routine needle biopsy procedure multiple samples at different depths are acquired to avoid sampling bias or negative histology. With the in situ optical guidance technique, as fluorescence is found, less tissue material is needed. In turn, this would decrease the risk of hemorrhagic complications as fewer cuts are made.[4] However, with an increased number of molecular analyses needed for diagnosis, the consideration of how much tissue to sample should be made in consultation with neuropathologists.

In addition to 5-ALA, surgical adjuncts such as robot assisted surgery and intraoperative imaging have been suggested to confirm correctness of the target position and increase safety compared to the routine neuronavigation procedure. Although studies show increased accuracy as robot assistance is used, only negligible changes in diagnostic yield and safety have been reported.[1] Additionally, as with the blue-light microscope, feedback is given after sampling.

Other Spectral Peaks

In addition to the well-documented PpIX peaks (635 nm, 704 nm) associated with high-grade brain tumor tissue, spectral peaks at wavelengths 580 nm and in the 620–630 nm range were found in the presented cohort. The 580 nm peaks were present in 4 patients (tumor and non-tumor) and have previously been attributed to lipofuscin.[33,34] Lipofuscin increase is typically associated with low-density margins of the tumor or healthy tissue. Peaks in the 620–630 nm, also referred to as blue-shifted peaks in relation to the PpIX peak, and their importance for tumor grading are currently being debated. Some groups assign these contributions to other porphyrins[28,33] and others suggest attribution to coproporphyrin III.[35] In this cohort, blue-shifted peaks were found for twelve patients. Peaks were found in proximity to the 635 nm peak and in one non-tumorous case where an increase of astrocytes, but no sign of malignancy, was found in the neuropathological analysis.

Objective Grading and Reduced Number of Trajectories

Optical guidance is commonly associated with fluorescence guidance during resections[11,12] where a subjective grading of "strong," "weak," or no fluorescence is used.[9,11,28] With a probe-based system, fluorescence spectra are measured in situ and shown in real time, eliminating the subjectivity of a visual grading system. In this study, the same 5-ALA dose as in FGR was used and no adverse events or side effects were found.

In total, 21 trajectories were probed in this study. One patient (Patient 1) had 2 trajectories with PpIX fluorescence present in both. The intraoperative neuropathological analysis showed marginal zone in the first sample; thus, a second trajectory was probed and a diagnosis could be posed. For one patient with non-tumor response (Patient 17), a second sample along the same trajectory was sampled. This sample also had a non-tumor response; thus, the surgery was closed. The number of trajectories are rarely reported, but can be compared to our previous study[19] where frame-based needle biopsy was carried out in a 20-patient cohort. In the Richter and colleagues study, 28 trajectories were probed with up to 3 trajectories in some patients. Additionally, optical measurements were made with the probe before insertion of the biopsy needle. Compared with this study, where the probe was integrated into the biopsy needle and only one insertion was required, the number of trajectories was markedly reduced.

Microcirculation and Relative Location

High-grade tumors are associated with an abundance of (pathological) blood vessels, and as the tissue is cut, bleeding is most likely unavoidable in relation to tissue sampling. However, we have previously shown that 0.5–1 mm steps of tissue microcirculation can act as a "vessel-alarm."[18,36] Thus, suggesting that sites of increased blood flow can be identified and sampling there potentially avoided. In the current study, increased microcirculation was found in 9 patients. Five patients (1, 6, 12, 16, and 17) had relative increases in the cortical region, 6 (6, 9, 10, 12, 16, 20) in the tumor region, one (9) in the vicinity of the lateral ventricle, and one (15) along the tentorium (Figure 4). Previous studies have found increased microcirculation in cortical regions and the vicinity of the lateral ventricle.[37] Rejmstad and colleagues also found increased microcirculation in tumorous regions.[38] Postoperative imaging revealed bleeding in 5 out of the 9 patients (asymptomatic, 6, 9, 12, 15, 17 or symptomatic, 6), and in an additional 5 patients (asymptomatic, 4, 5, 7, 8, 14). In 9 of the patients, bleedings were related to the biopsy location, one to the subarachnoid space, and one (also present in the biopsy group) superficial. As the steps between measurement sites during needle insertion were longer than in the previous study, all positions corresponding to increased microcirculation might not have been detected.

The incidence of asymptomatic bleeding in this patient cohort was within previously reported values[1,14,15] but at the higher end of the range. As has been stated previously, not all studies report on asymptomatic hemorrhages, and several clinics do not have a postoperative image as follow-up without a clinical indication, such as apparent bleeding during the surgical procedure. Therefore, more detailed investigations of bleeding incidence were not conducted. A symptomatic bleeding occurred in one patient causing a discrete restriction of the contralateral visual field. The diffuse tumor (formerly known as gliomatosis cerebri) was located in the temporomedial area in splenium and trigonum.

Cerebral tissue gray-whiteness measured through TLI indicates relative light intensity. Rejmstad et al. found a significant decrease in TLI signal in gray matter and tumor tissue compared to white matter.[38] These findings are corroborated by the overall trends found in this study.

Limitations

As comparisons are made across techniques, the resolutions of the different modalities should be considered. Here, the resolution varies from 3 µm slices for neuropathology to an 8 mm biopsy window during sampling. The penetration depth of the laser light varies for different tissues, for example, the 405 nm laser penetrates deeper in white matter compared to the denser glioma tissue.[3] Also, in the near-UV spectral region, absorption of blood is high. This was seen through decreased SNR as several spectra were affected by blood. In 8 out of 21 trajectories, the probe-needle kit was taken out and rinsed due to blood interference in the signal, before reinsertion along the same trajectory as previously, locked by the AutoGuide®. For the

780 nm laser (LDF), Monte Carlo simulations suggest sampling depth in the range of about 1 mm.[39,40]

Furthermore, during needle insertion, steps between measurement positions varied from 1 to 14 mm. The larger step size can lead to unidentified sites of increased microcirculation along the trajectory. In previous studies with frame-based biopsy, an in-house developed mechanical insertion device was used.[19] During the frameless procedure with the Autoguide®, implementation of a similar solution was not possible without severely limiting the available trajectory length. Thus, no mechanical insertion device was used.

Although this is a prospective study, the data was collected from a single center, resulting in a limited patient cohort. To further explore the potential of integrated optical guidance, future multi-center studies are warranted where the certainty and safety are compared to that of the routine procedure in a larger patient cohort.

Conclusions

Through in situ optical guidance, real-time feedback is given before tissue sampling, increasing certainty and precision in diagnostic tissue during frameless brain tumor biopsies. This study strengthens the previously proposed independence from intraoperative neuropathology as PpIX fluorescence is detected. Compared to previous studies, fewer trajectories were used, indicating reduced operation time and shorter time under anesthesia for the patient. The multiparametric analysis also suggests a detection limit for PpIX fluorescence in relation to Ki67 index, however, larger cohort studies are warranted for confirmation.

Supplementary material

Supplementary material is available online at *Neuro-Oncology Advances* (https://academic.oup.com/noa).

Keywords

5-aminolevulinic acid | digital pathology | glioblastoma | microcirculation | neuronavigation

Lay summary

Taking samples from brain tumors can be risky, and sometimes patients do not receive a complete diagnosis because surgeons may have not sampled the right part of the tumor. The authors of this study wanted to see if they could use tools that provide real-time feedback during biopsies to help surgeons locate the abnormal areas better. To do this, they used a tool that analyzes the reaction of light with different tissues, and they tested this on 20 patients. The results showed that this tool helped identify the right areas of the tumor to sample and reduced the number of times a biopsy was attempted.

Funding

This project is financially supported by the Swedish Foundation for Strategic Research (grant number RMX18-0056).

Acknowledgments

The authors are grateful to the clinical staff at the Departments of Neurosurgery and Clinical Pathology at Linköping University Hospital for their support during the study.

Conflict of interest statement

K.W. and J.R. have shares in university spin-off company FluoLink AB. E.K., P.M., and M.H. have no conflicts of interest to disclose.

Authorship statement

Experimental design: E.K., J.R., K.W.; Implementation: E.K., J.R., P.M., M.H., K.W.; Analysis: E.K., M.H.; Interpretation: E.K., J.R., K.W.; Writing: E.K., J.R., M.H., K.W.; Revision: E.K., J.R., P.M., M.H., K.W.

Data availability

Due to privacy reasons, the MRI data that support the findings in this study are not openly available. The anonymized optical data are available upon reasonable request. Data are stored under controlled access at Linköping University.

Affiliations

Department of Biomedical Engineering, Linköping University, Linköping, Sweden (E.K., J.R., K.W.); Department of Neurosurgery in Linköping, Linköping University, Linköping, Sweden (J.R., P.M.); Department of Biomedical and Clinical Sciences, Linköping University, Linköping, Sweden (P.M., M.H.); Department of Clinical Pathology in Linköping, Linköping University, Linköping, Sweden (M.H.)

References

1. Bex A, Mathon B. Advances, technological innovations, and future prospects in stereotactic brain biopsies. *Neurosurg Rev.* 2022;46(1):5.
2. Livermore LJ, Ma R, Bojanic S, Pereira EA. Yield and complications of frame-based and frameless stereotactic brain

biopsy--the value of intra-operative histological analysis. *Br J Neurosurg.* 2014;28(5):637–644.
3. Lu H, Grygoryev K, Bermingham N, et al. Combined autofluorescence and diffuse reflectance for brain tumour surgical guidance: initial ex vivo study results. *Biomed Opt Express.* 2021;12(4):2432–2446.
4. von Campe G, Moschopulos M, Hefti M. 5-Aminolevulinic acid-induced protoporphyrin IX fluorescence as immediate intraoperative indicator to improve the safety of malignant or high-grade brain tumor diagnosis in frameless stereotactic biopsies. *Acta Neurochir (Wien).* 2012;154(4):585–8; discussion 588.
5. Widhalm G, Minchev G, Woehrer A, et al. Strong 5-aminolevulinic acid-induced fluorescence is a novel intraoperative marker for representative tissue samples in stereotactic brain tumor biopsies. *Neurosurg Rev.* 2012;35(3):381–91; discussion 391.
6. Khatab S, Spliet W, Woerdeman PA. Frameless image-guided stereotactic brain biopsies: emphasis on diagnostic yield. *Acta Neurochir (Wien).* 2014;156(8):1441–1450.
7. Skyrman S, Burström G, Lai M, et al. Diffuse reflectance spectroscopy sensor to differentiate between glial tumor and healthy brain tissue: a proof-of-concept study. *Biomed Opt Express.* 2022;13(12):6470–6483.
8. Thien A, Han JX, Kumar K, et al. Investigation of the usefulness of fluorescein sodium fluorescence in stereotactic brain biopsy. *Acta Neurochir (Wien).* 2018;160(2):317–324.
9. Millesi M, Kiesel B, Wöhrer A, et al. Is intraoperative pathology needed if 5-aminolevulinic-acid-induced tissue fluorescence is found in stereotactic brain tumor biopsy? *Neurosurgery.* 2020;86(3):366–373.
10. Shofty B, Richetta C, Haim O, et al. 5-ALA-assisted stereotactic brain tumor biopsy improve diagnostic yield. *Eur J Surg Oncol.* 2019;45(12):2375–2378.
11. Hadjipanayis CG, Stummer W, Sheehan JP. 5-ALA fluorescence-guided surgery of CNS tumors. *J Neurooncol.* 2019;141(3):477–478.
12. Richter JCO, Haj-Hosseini N, Hallbeck M, Wårdell K. Combination of handheld probe and microscopy for fluorescence guided surgery in the brain tumor marginal zone. *Photodiagnosis Photodyn Ther.* 2017;18:185–192.
13. Haj-Hosseini N, Richter JCO, Milos P, Hallbeck M, Wårdell K. 5-ALA fluorescence and laser Doppler flowmetry for guidance in a stereotactic brain tumor biopsy. *Biomed Opt Express.* 2018;9(5):2284–2296.
14. Riche M, Amelot A, Peyre M, et al. Complications after frame-based stereotactic brain biopsy: a systematic review. *Neurosurg Rev.* 2021;44(1):301–307.
15. Riche M, Marijon P, Amelot A, et al. Severity, timeline, and management of complications after stereotactic brain biopsy. *J Neurosurg.* 2022;136(3):867–876.
16. Goyette A, Pichette J, Tremblay MA, et al. Sub-diffuse interstitial optical tomography to improve the safety of brain needle biopsies: a proof-of-concept study. *Opt Lett.* 2015;40(2):170–173.
17. Picot F, Goyette A, Obaid S, et al. Interstitial imaging with multiple diffusive reflectance spectroscopy projections for in vivo blood vessels detection during brain needle biopsy procedures. *Neurophotonics.* 2019;6(2):025003.
18. Wårdell K, Zsigmond P, Richter J, Hemm S. Relationship between laser Doppler signals and anatomy during deep brain stimulation electrode implantation toward the ventral intermediate nucleus and subthalamic nucleus. *Neurosurgery.* 2013;72(2 Suppl Operative):ons127–40; discussion ons140.
19. Richter J, Haj-Hosseini N, Milos P, Hallbeck M, Wårdell K. Optical brain biopsy with a fluorescence and vessel tracing probe. *Oper Neurosurg (Hagerstown).* 2021;21(4):217–224.
20. Wårdell K, Klint E, Milos P, Richter J. One-insertion stereotactic brain biopsy using in vivo optical guidance-a case study. *Oper Neurosurg (Hagerstown).* 2023;25(2):176–182.
21. Klint E, Richter J, Wårdell K. Combined use of frameless neuronavigation and in situ optical guidance in brain tumor needle biopsies. *Brain Sciences.* 2023;13(5):809.
22. Klint E, Mauritzon S, Ragnemalm B, Richter J, Wårdell K. FluoRa - a system for combined fluorescence and microcirculation measurements in brain tumor surgery. *Annu Int Conf IEEE Eng Med Biol Soc.* 2021;2021:1512–1515.
23. WHO Classification of Tumours Editorial Board. *Central nervous system tumours.* Vol 6. 5 ed. Lyon, France: International Agency for Research on Cancer; 2021.
24. Bodén ACS, Molin J, Garvin S, et al. The human-in-the-loop: an evaluation of pathologists' interaction with artificial intelligence in clinical practice. *Histopathology.* 2021;79(2):210–218.
25. Evers G, Kamp M, Warneke N, et al. 5-Aminolaevulinic acid-induced fluorescence in primary central nervous system lymphoma. *World Neurosurg.* 2017;98:375–380.
26. Kiesel B, Millesi M, Woehrer A, et al. 5-ALA-induced fluorescence as a marker for diagnostic tissue in stereotactic biopsies of intracranial lymphomas: experience in 41 patients. *Neurosurg Focus.* 2018;44(6):E7.
27. Jaber M, Wölfer J, Ewelt C, et al. The value of 5-aminolevulinic acid in low-grade gliomas and high-grade gliomas lacking glioblastoma imaging features: an analysis based on fluorescence, magnetic resonance imaging, 18F-Fluoroethyl tyrosine positron emission tomography, and tumor molecular factors. *Neurosurgery.* 2016;78(3):401–411; discussion 411.
28. Black D, Kaneko S, Walke A, et al. Characterization of autofluorescence and quantitative protoporphyrin IX biomarkers for optical spectroscopy-guided glioma surgery. *Sci Rep.* 2021;11(1):20009.
29. Valdés PA, Kim A, Brantsch M, et al. δ-aminolevulinic acid-induced protoporphyrin IX concentration correlates with histopathologic markers of malignancy in human gliomas: the need for quantitative fluorescence-guided resection to identify regions of increasing malignancy. *Neuro Oncol.* 2011;13(8):846–856.
30. Fontana AO, Piffaretti D, Marchi F, et al. Epithelial growth factor receptor expression influences 5-ALA induced glioblastoma fluorescence. *J Neurooncol.* 2017;133(3):497–507.
31. Wen PY, Weller M, Lee EQ, et al. Glioblastoma in adults: a Society for Neuro-Oncology (SNO) and European Society of Neuro-Oncology (EANO) consensus review on current management and future directions. *Neuro Oncol.* 2020;22(8):1073–1113.
32. Louis DN, Perry A, Wesseling P, et al. The 2021 WHO Classification of Tumors of the Central Nervous System: a summary. *Neuro Oncol.* 2021;23(8):1231–1251.
33. Alston L, Mahieu-Williame L, Hebert M, et al. Spectral complexity of 5-ALA induced PpIX fluorescence in guided surgery: a clinical study towards the discrimination of healthy tissue and margin boundaries in high and low grade gliomas. *Biomed Opt Express.* 2019;10(5):2478–2492.
34. Mehidine H, Chalumeau A, Poulon F, et al. Optical signatures derived from deep UV to NIR excitation discriminates healthy samples from low and high grades glioma. *Sci Rep.* 2019;9(1):8786.
35. Suero Molina E, Black D, Walke A, et al. Unraveling the blue shift in porphyrin fluorescence in glioma: the 620 nm peak and its potential significance in tumor biology. *Front Neurosci.* 2023;17:1261679.
36. Wårdell K, Hemm-Ode S, Rejmstad P, Zsigmond P. High-resolution laser doppler measurements of microcirculation in the deep brain structures: a method for potential vessel tracking. *Stereotact Funct Neurosurg.* 2016;94(1):1–9.
37. Zsigmond P, Hemm-Ode S, Wårdell K. Optical measurements during deep brain stimulation lead implantation: safety aspects. *Stereotact Funct Neurosurg.* 2017;95(6):392–399.
38. Rejmstad P, Åkesson G, Åneman O, Wårdell K. A laser doppler system for monitoring cerebral microcirculation: implementation and evaluation during neurosurgery. *Med Biol Eng Comput.* 2016;54(1):123–131.
39. Johansson J, Fredriksson I, Wårdell K, Eriksson O. Simulation of reflected light intensity changes during navigation and radio-frequency lesioning in the brain. *J Biomed Opt.* 2009;14(4):044040.
40. Qian Z, Victor S, Gu Y, Giller C, Liu H. Look-ahead distance of a fiber probe used to assist neurosurgery: phantom and monte carlo study. *Opt Express.* 2003;11(16):1844–1855.